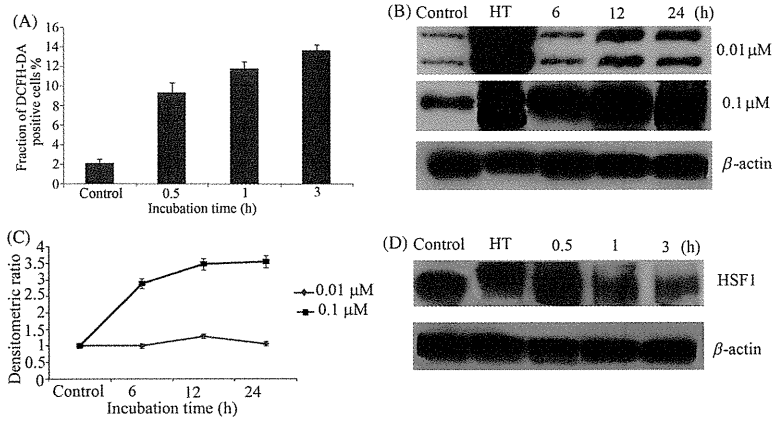

Figure 3. (A) U937 cells were first incubated with DCFH-DA for 30 min and then treated with shikonin in a time-dependent manner. Intracellular peroxide level was measured by flow cytometry. (B) Concentration and time-dependent induction of Hsp70 was measured by western blotting. Hyperthermia (HT) 44°C for 15 min was used as a positive control. (C) Bands were quantified by densitometry and normalised with β-actin. Bars indicate standard deviation ($n = 3$). (D) HSF1 phosphorylation was measured time-dependently by western blotting. Hyperthermia (HT) 44°C for 15 min was used as a positive control.

treated with 0.1 μM shikonin in a time-dependent manner followed by western blot analysis.

Phosphorylation of HSF1 is usually detected as an upward band shift [20]. No upward band shift was observed after shikonin treatment till 3 h, while very clear upward shift was observed in HT-treated cells. This result indicates that HSF1 is not playing a role in shikonin-induced HSP up-regulation (Figure 3D).

Identification of genes responsive to shikonin treatment

As shikonin treatment did not show the activation of HSF1, we carried out gene chip analysis of cells treated with or without shikonin after 3 h incubation. Many probe sets were differentially expressed by >2-fold in cells treated with the compound, 277 up-regulated and 262 down-regulated in comparison to control. The complete list of genes from all samples is available on the Gene Expression Omnibus (http://www.ncbi.nlm.nih.gov/geo/query/acc.cgi?acc=GSE24743). The biologically relevant functions and networks of the up-regulated probe sets obtained from the gene chip analysis were identified using Ingenuity Pathways Knowledge Base. Of 277 up-regulated probe sets analysed, 77 genes were functionally annotated. On the basis of significance, the top three molecular functions were cellular compromise (p value: 3.73E-12 to 2.68E-02), cellular function and maintenance (3.73E-12 to 4.65E-02), and post-transcriptional modification (1.36E-7 to 3.34E-02). As shown in Figure 4, a significant gene network contained HSP-related genes such as HSPA1A (heat shock 70 kDa protein 1A), HSPA6 (heat shock 70 kDa protein 6) and DNAJA1 (DnaJ (Hsp40) homologue, subfamily A, member 1) and Nrf2(NFE2L2)-target genes such as HMOX1 (heme oxygenase (decycling) 1), NQO1 (NAD(P)H dehydrogenase, quinone 1) and SQSTM1 (sequestosome 1). To confirm the results of gene chip analysis, a real-time qPCR assay was performed for four selected genes in the network. As we expected, the expression levels of these genes were significantly increased by the treatment (Figure 5).

Discussion

Toward the goal of developing novel cytoprotective agents we did screening of 80 chemical compounds isolated from medicinal plants for their HSP-inducing activities. Among the five active Hsp70 inducers, shikonin was most potent. Shikonin is a chemical compound isolated from the root of a plant *Lithospermum erythrorhizon*. It is known to have antibacterial [21], antifungal [21], anti-human immunodeficiency virus [22], anticancer [23] and anti-inflammatory activity [23]. But to our knowledge there is no report on its ability to induce HSP up-regulation.

Several chemical compounds are known to induce HSP through the activation of HSF1 [11]. In this study, after shikonin treatment significant Hsp70 up-regulation was observed without the activation

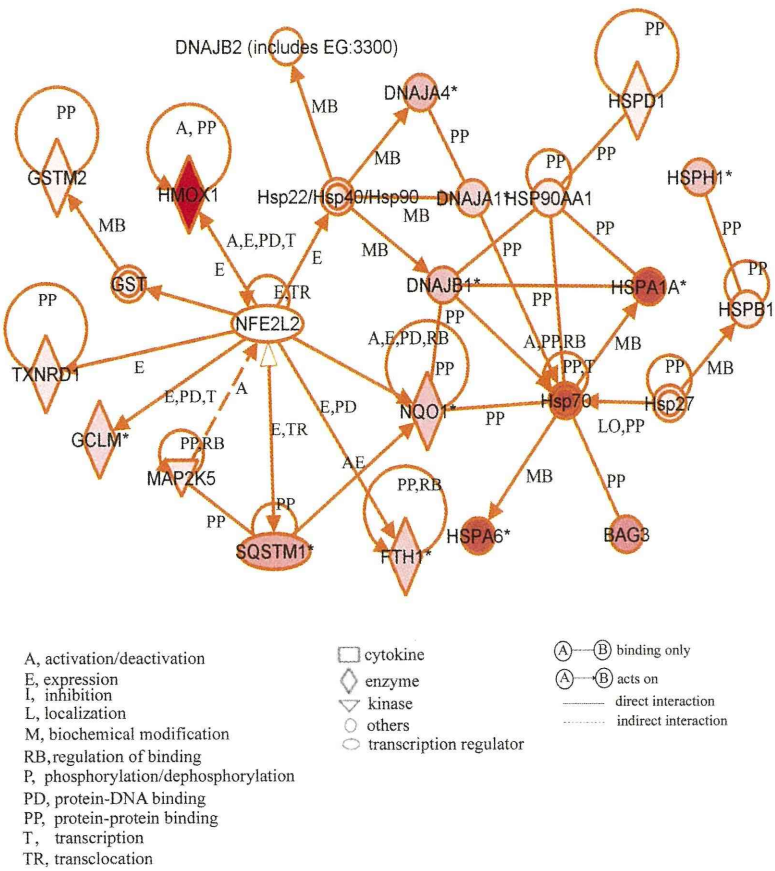

Figure 4. A gene network including up-regulated genes. Cells were treated with the compound and cultured at 37°C for 3 h. Gene chip analysis was performed. Genes that were up-regulated were analysed using Ingenuity Pathways Analysis tools. The network is displayed graphically as nodes (genes or protein group) and edges (the biological relationships between the nodes). The node colour of genes indicated the expression level of genes. Nodes and edges are displayed in various shapes and labels that present the functional class of genes and the nature of the relationship between the nodes, respectively.

of HSF1. With the high-density oligonucleotide microarrays and computational gene expression tools we identified a unique gene network containing HSPs and Nrf2-target genes. Nrf2 is an antioxidant transcription master regulator and belongs to the cap 'n' collar family of transcription factors. Small Maf proteins (MafF, MafG and MafK) possess the region-leucine zipper (L-Zip) domain that is required for homodimer or heterodimer complex formation with other basic L-Zip transcription factors such as Nrf2 [24]. Nrf2 is sequestered in cytoplasm by its repressor Keap1, released and translocated into the nucleus under oxidative stress [25]. In the nucleus, the heterodimer complex of Nrf2 and small Maf proteins binds to the antioxidant-responsive element (ARE) sequence leading to transcriptional activation of downstream genes encoding phase II detoxifying enzymes, antioxidants [26] and chaperone proteins [27].

Almeida et al. [28] recently indicated that Hsp70 expression is regulated by an ARE/EpRE sequence in a Zebrafish model. In many studies, Nrf2 have been reported to induce different Hsps [27, 29–31] and in one study, Hsp70 was specifically up-regulated in mouse liver in wild-type but not knockout mice [29]. Furthermore, it has also been reported that activation of Nrf2 increases expression of Hsp40 [27]. In addition, several studies reported a concomitant induction of Hsp70 and Nrf2-regulated gene HMOX1 by electrophiles [32].

Although the detailed mechanisms by which shikonin induces protein expression of Hsp70 are not fully understood, Nrf2 and its target genes may have participated in the up-regulation of Hsp70 in

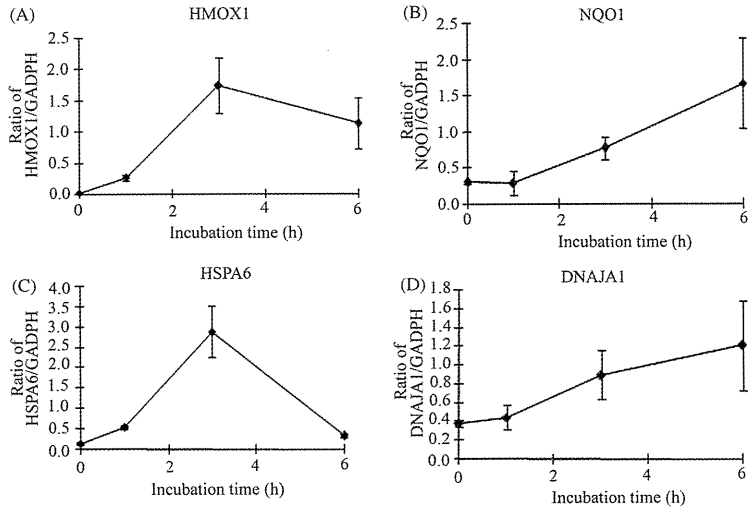

Figure 5. Verification of microarray results by qPCR assay. Cells were treated with 0.1 μM shikonin time-dependently and then real-time qPCR assay was performed. (A) HMOX1 (heme oxygenase (decycling) 1) (B) NQO1 (NAD(P)H dehydrogenase, quinone 1) (C) HSPA6 (heat shock 70 kDa protein 6) (D) DNAJA1(DnaJ (Hsp40) homologue, subfamily A, member 1). Each mRNA expression level was normalised with GADPH. Data are presented as mean ± SD ($n = 3$).

U937 cells. The elucidation of the molecular mechanism to induce Hsp70 by shikonin remains for further investigation in the future.

Declaration of interest: This work was supported by the Expansion Program, Regional Innovation Cluster Program, Global Type (II) from the Ministry of Education, Culture, Sports, Science and Technology, Japan, and by research grants from the Smoking Research Foundation (TK, TY) and the International Association of Sensitization for Cancer Treatment (IASCT)(KA). The authors alone are responsible for the content and writing of the paper.

References

1. Giudice A, Arra C, Turco MC. Review of molecular mechanisms involved in the activation of the Nrf2-ARE signaling pathway by chemopreventive agents. Methods Mol Biol 2010;647:37–74.
2. Calabrese V, Mancuso C, Sapienza M, Puleo E, Calafato S, Cornelius C, et al. Oxidative stress and cellular stress response in diabetic nephropathy. Cell Stress Chaperones 2007;12:299–306.
3. Calabrese V, Mancuso C, Ravagan A, Perluigi M, Cini C, De Macro C, et al. Oxidative stress redox hemostasis and cellular stress response in Ménière's disease: Role of vitagenes. J Neurochem 2007;10:709–717.
4. Calabrese V, Cornelius C, Maiolino L, Luca M, Chiaramonte R, Toscano MA, Serra A. Neurochem Res 2010;35:2208–2217.
5. Schlesinger MJ, Ashburner M, Tissieres A. Heat Shock from Bacteria to Man. New York: Cold Spring Harbor; 1982.
6. Lanneau D, Brunet M, Frisan E, Solary E, Fontenay M, Garrido C. Heat shock proteins: Essential proteins for apoptosis regulation. J Cell Mol Med 2008;12:743–761.
7. Ohtsuka K, Kawashima D, Asai M. Dual functions of heat shock proteins: Molecular chaperones inside of cells and danger signals outside of cells. Thermal Med 2007;23:11–22.
8. Otani S, Otaka M, Jin M, Okuyama A, Itoh S, Iwabuchi A, et al. Effect of preincubation of heat shock proteins on acetic acid-induced colitis in rats. Dig Dis Sci 1997;42:833–846.
9. Rokutan K, Hirakawa T, Teshima S, Nakano Y, Miyoshi M, Kawai T, et al. Implications of heat shock/stress proteins for medicine and disease. J Med Invest 1998;44:137–147.
10. Kobayashi Y, Kume A, Li M, Doyu M, Hata M, Ohtsuka K, et al. Chaperones Hsp70 and Hsp40 suppress aggregate formation and apoptosis in cultured neuronal cells expressing truncated androgen receptor protein with expended polyglutamine tract. J Biol Chem 2000;275:8772–8778.
11. Yan D, Saito K, Ohmi Y, Fujie N, Ohtsuka K. Paeoniflorin, a novel heat shock protein-inducing compound. Cell Stress Chaperones 2004;9:378–389.
12. Genc K, Egrilmez YM, Genc S. Erythropoietin induces nuclear translocation of Nrf2 and heme oxygenase-1 expression in SH-SY5Y cells. Cell Biochem Funct 2010;28:197–201.
13. Ahmed K, Matsuya Y, Nemoto H, Zaidi SF, Sugiyama T, Yoshihisa Y, et al. Mechanism of apoptosis induced by a newly synthesized derivative of macrosphelides with a thiazole side chain. Chem Biol Interact 2008;117:218–226.
14. Tabuchi Y, Takasaki I, Zhao QL, Wada S, Hori T, Feril LB, et al. Genetic networks responsive to low-intensity pulsed ultrasound in human lymphoma U937 cells. Cancer Lett 2008;270:286–294.
15. Hori T, Kondo T, Tabuchi Y, Takasaki I, Zhao QL, Kanamori M, et al. Molecular mechanism of apoptosis and gene expressions in human lymphoma U937 cells treated with anisomycin. Chem Biol Interact 2007;172:125–140.

16. Tabuchi Y, Takasaki I, Doi T, Ishii Y, Sakai H, Kondo T. Genetic networks responsive to sodium butyrate in colonic epithelial cells. FEBS Lett 2006;580:3035–3041.
17. Salunga TL, Tabuchi Y, Takasaki I, Feril Jr LB, Zhao QL, Ohtsuka K, et al. Identification of genes responsive to paeoniflorin, a heat shock protein-inducing compound, in human leukaemia U937 cells. Int J Hyperthermia 2007;23:529–537.
18. Mao X, Yu CR, Li WH, Li WX. Induction of apoptosis by shikonin through a ROS/JNK-mediated process in Bcr/Abl-positive chronic myelogenous leukemia (CML) cells. Cell Res 2008;18:879–88.
19. Calderwood SK. Heat shock proteins in breast cancer progression – A suitable case for treatment? Int J Hyperthermia 2010;26:681–685.
20. Sarge KD, Murphy SP, Morimoto RI. Activation of heat shock gene transcription by heat shock factor 1 involves oligomerization, acquistion of DNA binding activity, and nuclear localization and can occur in the absence of stress. Mol Cell Biol 1993;13:1392–1407.
21. Brigham LA, Michaels PJ, Flores HE. Cell-specific production and antimicrobial activity of naphthoquinones in roots of *Lithospermum erythrorhizon*. Plant Physiol 1999;119:417–428.
22. Chen X, Yang L, Zhang N, Turpin JA, Buckheit RW, Osterling C, et al. Shikonin, a component of Chinese herbal medicine, inhibits chemokine receptor function and suppresses human immunodeficiency virus type 1. Antimicrob Agents Chemother 2003;47:2810–2816.
23. Chen X, Yang L, Oppenheim JJ, Howard MZ. Cellular pharmacological study of shikonin derivatives. Phytother Res 2002;16:199–209.
24. Motohashi H, O'Connor T, Katsuoka F, Engel JD, Yamamoto M. Integration and diversity of the regulatory network composed of Maf and CNC families of transcription factors. Gene 2002;294:1–12.
25. Itoh K, Chiba T, Takahashi S, Ishii T, Igarashi K, Katoh Y, et al. An Nrf2/small Maf heterodimer mediates the induction of phase II detoxifying enzyme genes through antioxidant response elements. Biochem Biophys Res Commun 1997;236:313–322.
26. Itoh K, Wakabayashi N, Katoh Y, Ishii T, Igarashi K, Engel JD, et al. Keap1 represses nuclear activation of antioxidant responsive elements by Nrf2 through binding to the amino-terminal Nef2 domain. Genes Dev 1999;13:76–86.
27. Kwak MK, Wakabayashi N, Itoh K, Motohashi H, Yamamoto M, Kensler TW. Modulation of gene expression by cancer chemopreventive dithiolethiones through Keap1-Nrf2 pathway. J Biol Chem 2003;278:8135–8145.
28. Almeida DV, Nornberg BF, Geracitano LA, Barros DM, Monserrat JM, Marins LF. Induction of phase II enzymes and hsp70 genes by copper sulfate through the electrophile-responsive element (EpRE): Insights obtained from a transgenic zebrafish model carrying an orthologous EpRE sequence of mammalian origin. Fish Physiol Biochem 2009; 36:347–353.
29. Hu R, Xu C, Shen G, Jain MR, Khor TO, Gopalkrishnan A, et al. Identification of Nrf2-regulated genes induced by chemopreventive isothiocyanate PEITC by oligonucleotide microarray. Life Sci 2006;79:1944–1955.
30. Nair S, Li W, Kong AN. Natural dietary anti-cancer chemopreventive compounds: Redox-mediated differential signaling mechanisms in cytoprotection of normal cells versus cytotoxicity in tumor cells. Acta Pharmacol Sin 2007;28:459–472.
31. Thimmulappa RK, Mai KH, Srisuma S, Kensler TW, Yamamoto M, Biswal S. Identification of Nrf2-regulated genes induced by the chemopreventive agent sulforaphane by oligonucleotide microarray. Cancer Res 2002;62:5196–5203.
32. Thompson CA, Burcham PC. Genome-wide transcriptional responses to acrolein. Chem Res Toxicol 2008;12:2245–2256.

Toxicon 57 (2011) 1081–1092

Contents lists available at ScienceDirect

Toxicon

journal homepage: www.elsevier.com/locate/toxicon

Chemical and biological characterization of four new linear cationic α-helical peptides from the venoms of two solitary eumenine wasps

Marisa Rangel [a], Marcia Perez dos Santos Cabrera [b], Kohei Kazuma [c], Kenji Ando [c], Xiaoyu Wang [c], Manabu Kato [d], Ken-ichi Nihei [e], Izaura Yoshico Hirata [f], Tyra J. Cross [g], Angélica Nunes Garcia [a], Eliana L. Faquim-Mauro [a], Marcia Regina Franzolin [h], Hiroyuki Fuchino [i], Kanami Mori-Yasumoto [j], Setsuko Sekita [j], Makoto Kadowaki [c], Motoyoshi Satake [c], Katsuhiro Konno [c,*]

[a] *Immunopathology Laboratory, Butantan Institute, Sao Paulo, SP 05503-900, Brazil*
[b] *Department of Physics, IBILCE, São Paulo State University, São José do Rio Preto, SP 15054-000, Brazil*
[c] *Institute of Natural Medicine, University of Toyama, 2630 Sugitani, Toyama 930-0194, Japan*
[d] *Yamada Apiculture Center, Inc., Kagamino, Okayama 708-0393, Japan*
[e] *Faculty of Agriculture, Utsunomiya University, Utsunomiya, Tochigi 321-8505, Japan*
[f] *Department of Biophysics, Paulista Medical School, Federal University of São Paulo, São Paulo, SP 04044-020, Brazil*
[g] *Genome B.C. Proteomics Centre, University of Victoria, Victoria, British Columbia V8Z 7X8, Canada*
[h] *Bacteriology Laboratory, Butantan Institute, Sao Paulo, SP 05503-900, Brazil*
[i] *Research Center for Medicinal Plant Resources, National Institute of Biomedical Innovation, Tsukuba, Ibaraki 305-0843, Japan*
[j] *Faculty of Pharmaceutical Sciences at Kagawa Campus, Tokushima Bunri University, Sanuki, Kagawa 769-2193, Japan*

ARTICLE INFO

Article history:
Received 1 February 2011
Received in revised form 13 April 2011
Accepted 19 April 2011
Available online 29 April 2011

Keywords:
Solitary wasp
Linear cationic α-helical peptide
Amphipathic α-helix structure
Antimicrobial activity

ABSTRACT

Four novel peptides were isolated from the venoms of the solitary eumenine wasps *Eumenes rubrofemoratus* and *Eumenes fraterculus*. Their sequences were determined by MALDI-TOF/TOF (matrix assisted laser desorption/ionization time-of-flight mass spectrometry) analysis, Edman degradation and solid-phase synthesis. Two of them, eumenitin-R (LNLKGLIKKVASLLN) and eumenitin-F (LNLKGLFKKVASLLT), are highly homologous to eumenitin, an antimicrobial peptide from a solitary eumenine wasp, whereas the other two, EMP-ER (FDIMGLIKKVAGAL-NH_2) and EMP-EF (FDVMGIIKKIAGAL-NH_2), are similar to eumenine mastoparan-AF (EMP-AF), a mast cell degranulating peptide from a solitary eumenine wasp. These sequences have the characteristic features of linear cationic cytolytic peptides; rich in hydrophobic and basic amino acids with no disulfide bond, and accordingly, they can be predicted to adopt an amphipathic α-helix secondary structure. In fact, the CD (circular dichroism) spectra of these peptides showed significant α-helical conformation content in the presence of TFE (trifluoroethanol), SDS (sodium dodecylsulfate) and asolectin vesicles. In the biological evaluation, all the peptides exhibited a significant broad-spectrum antimicrobial activity, and moderate mast cell degranulation and leishmanicidal activities, but showed virtually no hemolytic activity.

1. Introduction

Solitary wasps are known to inject their venoms into insects or spiders, paralyzing the prey in order to feed their larvae. Therefore, the solitary wasp venoms should contain a variety of neurotoxins acting on nervous systems. In fact,

Abbreviations: MALDI-TOF MS, matrix assisted laser desorption/ionization time-of-flight mass spectrometry; CD, circular dichroism; TFE, trifluoroethanol; SDS, sodium dodecylsulfate; PC, L- -phosphatidylcholine; PG, L- -phosphatidyl-DL-glycerol; HEPES, (N-[2-hydroxyethyl]piperazine-N -[2-ethanesulfdonic acid]; PBS, phosphate buffered saline.

* Corresponding author. Tel.: +81 76 434 7605; fax: +81 76 434 5055.
E-mail address: kkgon@inm.u-toyama.ac.jp (K. Konno).

0041-0101/$ – see front matter © 2011 Elsevier Ltd. All rights reserved.
doi:10.1016/j.toxicon.2011.04.014

polyamine toxins (Eldefrawi et al., 1988), peptide neurotoxins (Yasuhara et al., 1987; Konno et al., 1998) and a protein paralyzing toxin (Yamamoto et al., 2007) have so far been found in several solitary wasp venoms. Besides the neurotoxins, we have found that cytolytic peptides are also present in the solitary wasp venoms. Eumenine mastoparan-AF (EMP-AF) was the first to be found (Konno et al., 2000; dos Santos Cabrera et al., 2004), having similar characteristics to those of mastoparan, a representative of the cytolytic peptides in social wasp venoms. Eumenitin is also homologous to mastoparan, but has an extra hydrophilic amino acid at the C-terminus without amide modification (Konno et al., 2006). Anoplin was isolated from spider wasp venom and is the smallest molecule in this type of peptides (Konno et al., 2001). Decoralin, another linear cationic α-helical peptide, has features similar to anoplin, but like EMP-AF *vs.* eumenitin, it has an extra hydrophilic amino acid without amide modification at the C-terminus (Konno et al., 2007). Except for anoplin, these cytolytic peptides were found in solitary eumenine wasps, alternatively called "mud dauber wasps" or "potter wasps", because they construct their pot-shaped nest with mud. Additionally, the eumenine wasps prey only on caterpillars, Lepidopteron larvae.

In our continuing survey of biologically active substances in solitary wasp venoms, we have isolated four new linear cationic α-helical peptides from two species of the eumenine solitary wasps, *Eumenes rubrofemoratus* and *Eumenes fraterculus*. Two of them, named eumenitin-R and eumenitin-F, are highly homologous to eumenitin, whereas the other two, named eumenine mastoparan-ER (EMP-ER) and eumenine mastoparan-EF (EMP-EF), are similar to EMP-AF, and thus, can be classified as mastoparan peptides. We now report the isolation, chemical characterization and biological evaluation of these novel peptides, including a secondary structure analysis and pore-forming activity.

2. Materials and methods

2.1. Purification

Female wasps of *E. rubrofemoratus* and *E. fraterculus* were collected at Yokohama, Kanagawa in Japan. The collected specimens were immediately frozen by dry ice and kept at −75 °C until use. The venom sacs were dissected immediately after being thawed and then lyophilized.

Fourteen lyophilized venom sacs of *E. rubrofemoratus* were extracted (5 × 1 mL) with 1:1 acetonitrile–water containing 0.1% TFA (CH_3CN/H_2O/0.1% TFA). The extract was lyophilized, re-dissolved in 50 μL of water and subjected to reversed-phase HPLC (Shimadzu Corp., Kyoto, Japan) using CAPCELL PAK C_{18}, 6 × 150 mm (SHISEIDO Co., Ltd., Tokyo, Japan) with linear gradient from 5% to 65% CH_3CN/H_2O/0.1% TFA at a flow rate of 1 mL/min over 30 min (Fig. 1A) to give eumenitin-R and EMP-ER eluted at 26.1 and 27.6 min, respectively.

Twenty lyophilized venom sacs of *E. fraterculus* were subjected to the same extraction procedure to give eumenitin-F and EMP-EF eluted at 26.2 and 29.0 min, respectively (Fig. 1B).

2.2. Mass spectrometry

All mass spectra were acquired on an Autoflex TOF/TOF mass spectrometer (Bruker Daltonics, Yokohama, Japan) equipped with 337 nm pulsed nitrogen laser under reflector mode. The accelerating voltage was 20 kV. Matrix, α-cyano-4-hydroxycinnamic acid (Aldrich), was prepared at a concentration of 10 mg/mL in 1:1 CH_3CN/0.1%TFA. External calibration was performed with [Ile^7]-angiotensin III (*m/z* 897.51, monoisotopic, Sigma) and human ACTH fragment 18–39 (*m/z* 2465.19, monoisotopic, Sigma). The sample solution (0.5 μL) dropped onto the MALDI sample plate was added to the matrix solution (0.5 μL) and allowed to dry at room temperature.

For TOF/TOF measurement, argon was used as a collision gas and ion was accelerated at 19 kV. The series of *b* and *y* ions were obtained which enabled identification of whole amino acid sequence by manual analysis.

2.3. Amino acid sequencing

Automated Edman degradation was performed by a gas-phase protein sequencer PPSQ-10 (Shimadzu Corp., Kyoto, Japan).

2.4. Peptide synthesis

The peptides were synthesized using Fmoc chemistry on a Prelude peptide synthesizer (Protein Technologies, Tucson, AZ) at a scale of 20 μmol. The synthesis of the peptide amides involved a 1 h offline swell of the Rink Amide MBHA resin in dichloromethane at room temperature prior to online synthesis. The peptide acids were synthesized using pre-loaded Wang resin. Subsequent residues, at a concentration of 100 mM, were double coupled using 20% piperidine as the deprotector and 1H-Benzotriazolium 1-[bis(dimethylamino)methylene]-5chloro-, hexafluorophosphate (1),3-oxide (HCTU) as the activator.

Cleavage was performed online with 95:2.5:2.5 TFA:-water:triisopropylsilane. The cleaved peptides were removed from the synthesizer and their TFA volumes were reduced under a stream of nitrogen. Ice cold ether was added to precipitate the peptides and after centrifugation at 13,000 rpm for 5 min, the ether layer was poured off. The pellets were resolubilized in 0.1% TFA and lyophilized (Modulyod, Thermo Savant).

The lyophilized pellets were resolubilized in 4 mL 12.5% acetonitrile, 0.1% TFA in water. Purification was carried out by reversed-phase HPLC Ultimate 3000 (Dionex, Sunnyvale, CA), monitoring peptide elution at 230 nm. Approximately 20 mg of the crude peptides were chromatographed using an Onyx Monolithic C_{18} column (10 × 100 mm, 13 nm & 2 μm pore size) with a linear gradient of 0.1% TFA in water (v/v) and 0.85% TFA in acetonitrile (v/v) at a flow rate of 5 mL/min over 25 min.

The fractions of interest were spotted onto a stainless steel MALDI plate and observed by MALDI-TOF (Applied Biosystems/MDS SCIEX, Foster City, CA). Fractions containing greater than 80% purity were pooled and lyophilized. The synthetic peptides were used in the assays below.

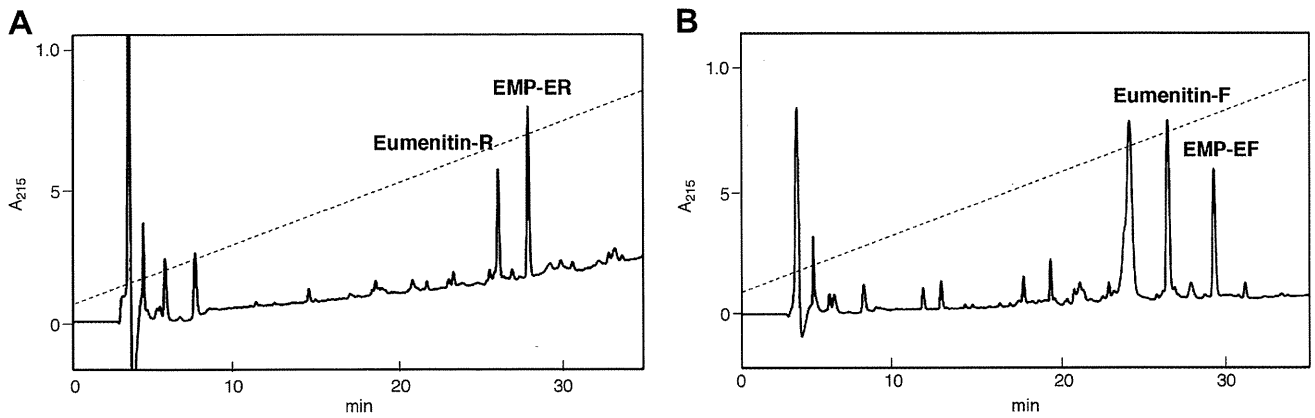

Fig. 1. Fractionation of venom extracts of (A) *Eumenes rubrofemoratus* and (B) *Eumenes fraterculus* by reverse-phase HPLC using CAPCELL PAK C_{18} (6 × 150 mm) with linear gradient of 5–65% CH_3CN/H_2O/0.1% TFA over 30 min at flow rate of 1 mL/min. UV absorption was monitored at 215 nm.

2.5. Circular dichroism (CD) spectroscopy

2.5.1. Small vesicles preparation (SUV)

Chloroform solution of asolectin was evaporated under N_2 flow, rendering homogeneous films on round bottom flasks that were further dried under vacuum for at least 3 h. Films were hydrated at room temperature with buffer (Tris/H_3BO_3 5 mM, 0.5 mM Na_2EDTA, 150 mM NaF, pH 7.5) to reach a final lipid concentration of 10 mg/mL and vortex mixed. SUVs were obtained after 50 min sonication (or until clear) with a tip sonicator in an ice/water bath, under N_2 flow; titanium debris was removed by centrifugation. SUVs were then submitted to 6 extrusions, at room temperature, through a 100 nm polycarbonate membrane followed by 11 extrusions through two stacked 50 nm polycarbonate membranes, using an Avanti mini-extruder. SUVs were kept under refrigeration and used in the same day of preparation.

2.5.2. CD spectroscopy experiments

CD spectra were obtained at 20 μM peptide concentration in different environments: bi-distilled water, 5 mM Tris/H_3BO_3 buffer, pH 7.5, 8 mM sodium dodecylsulfate (SDS) solution (above critical micelle concentration), 40% v/v trifluoroethanol (TFE)/water mixture, and in the presence of 100 and 250 μg/mL asolectin vesicles. TFE solutions are known inductors of helical structures and micellar SDS as well as vesicles are membrane mimetic environments with anionic character, a feature common to bacterial membranes (Yeaman and Yount, 2003). At 40% TFE or at micellar concentration of SDS solutions (8 mM) they tend to induce the maximum observable values (Prates et al., 2004). In the presence of asolectin vesicles saturation was found at 250 μg/mL concentration.

CD spectra were recorded from 260 to 203 or 190 nm (depending on signal-to-noise ratio) with a Jasco-710 spectropolarimeter (JASCO International Co. Ltd., Tokyo, Japan) which was routinely calibrated at 290.5 nm using *d*-10-camphorsulfonic acid solution. Spectra were acquired at 25 °C using 0.5-cm path length cell, averaged over eight scans, at a scan speed of 20 nm/min, bandwidth of 1.0 nm, 0.5 s response, and 0.2 nm resolution. Following baseline correction, the observed ellipticity, θ (mdeg), was converted to mean-residue ellipticity, [Θ] (deg cm^2/dmol), using the relationship $[\Theta] = 100\,\theta/(lcn)$ where '*l*' is the path length in centimeters, '*c*' is peptide milimolar concentration, and '*n*' the number of peptidic bonds. Assuming a two state model, the observed mean-residue ellipticity at 222 nm ($[\Theta]^{obs}{}_{222}$) was converted into α-helix fraction (f_H) using the method proposed by Rohl and Baldwin (1998) and previously described (Konno et al., 2001).

2.6. Channel-like incorporation in mimetic lipid bilayers

2.6.1. Bilayer formation

The lipid bilayers were obtained from giant unilamellar vesicles (GUVs), which were positioned onto the chip aperture by application of negative pressure. The GUVs burst as soon as they touch the glass surface of the chip and form a bilayer that spans the aperture (Sondermann et al., 2006). Asolectin (Sigma), a negatively charged mixture of lipids, was used to form artificial membranes. GUVs were formed by electroswelling, using the Nanion Technologies (Munich, Germany) device Vesicle Prep Pro©. 20 μL of 10 mg/mL lipid solution (in chloroform) were deposited onto an indium tin oxide (ITO) coated glass plate and evaporated for 45–60 min. A nitrile ring was placed around the dried lipid film and filled with 350 μL of 250 mM D-Sorbitol dissolved in Milli-Q water. A second ITO coated glass plate was placed on top of the ring. An AC voltage of 3 V peak-to-peak amplitude at 5 Hz frequency was supplied to the ITO slides over a period of 2 h at 36 °C (modified from Sondermann et al., 2006). The formed vesicles were kept in plastic vials under refrigeration (4 °C) until use or used immediately. GUVs suspensions were always observed under light microscope prior to use.

2.6.2. Electrophysiology

The experiments were performed with the automated Patch-Clamp device Port-a-Patch (Nanion Technologies – Munich, Germany), using borosilicate glass chips NPC-1 with aperture diameter of approximately 1 μm. The

resistance of the apertures was approximately 1–3 MΩ in 150 mM HCl solution. Current signals were amplified and recorded by an amplifier EPC-10 (Heka Elektronik, Lambrecht, Germany) and an analogical/digital interface ITC-1600. The system was computer controlled by the PatchControl™ software (Nanion) (Fertig et al., 2002; Sondermann et al., 2006).

During the experiments symmetrical solution of 150 mM HCl with 5 mM Tris was used. After a seal was formed (Rm > 500 mΩ), the peptides diluted with Milli-Q water at a 5 μM concentration were added to the *cis* side of the chip (top) to observe the single channel activity. The volume of peptide solution was never superior to 10% of the solution at the *cis* side. Voltage pulses were applied at the *trans* side of the chip (bottom). Usually, single channel activity started approximately 10 min after adding the peptides, as monitored by a constant V_{hold} of −100 mV. Single channel conductance of incorporated channels was determined under positive and negative voltage pulses. The experiments were performed at room temperature (~22 °C). The data was analyzed by PatchMaster and Matlab softwares.

2.7. Antimicrobial activity

The microorganisms used were: *Staphylococcus aureus* ATCC 25923, *Micrococcus luteus* ATCC 10240, *Staphylococcus epidermidis* (clinical sample), *Streptococcus pyogenes* (clinical sample), *Bacillus subtilis* ATCC 6633, *Escherichia coli* ATCC 25922, *Proteus mirabilis* (clinical sample), *Stenotrophomonas maltophilia* ATCC 13637, *Pseudomonas aeruginosa* ATCC 27853 and *Candida albicans* ATCC 90112.

The MICs of the tested peptides were determined by 2-fold serial broth microdilution in Müeller–Hinton broth (Difco) in 96-well plates. Aliquots of 45 μL of Müeller–Hinton broth (Difco) were placed in the microplates containing 50 μL of the peptides solutions. The mixture was completed by inoculation of 5 μL of bacterial suspension (10^7 CFU/mL), according NCCLS (Wayne, 2004), resulting in a final volume of 100 μL with 10^4 CFU/well. Following inoculation, the microtitre plates were incubated at 37 °C for 18 h before the results were recorded. After this time, the turbidity of the cultures was measured in an ELISA reader at 595 nm to assess bacterial growth. The results were expressed as inhibition percentage of optical density (OD) against a control; this control was obtained in each situation by measuring the OD of the microorganisms introduced into the plate in the absence of peptide. Also, the lowest concentration of peptide at which there is no visible growth after overnight incubation was observed.

2.8. Hemolytic activity

A 4% suspension of mouse erythrocytes (ES) was prepared as described (Rangel et al., 1997). Different concentrations of the peptides were incubated with the ES at room temperature (~22 °C) in an Elisa plate (96 wells). After 1 h it was centrifuged (1085× g/5 min), and the hemolytic activity of the supernatant was measured by the absorbance at 540 nm, considering as blank the absorbance of Krebs–Henseleit physiological solution (mM: NaCl 113; KH_2PO_4 1.2; KCl 4; $MgSO_4$ 1.2; $CaCl_2$ 2.5; $NaHCO_3$ 25; glucose 11.1), which was the vehicle for the peptides. Total hemolysis was obtained with 1% Triton X-100 and the percentage of hemolysis was calculated relative to this value.

2.9. Mast cell degranulation activity

The ability of the peptides to induce mast cells degranulation was investigated *in vitro* using the protocol of quantification of the granular enzyme β-hexosaminidase released in the supernatants of PT18 cells (a connective tissue-type mast cell model) and RBL-2H3 cells (a mucosal-type mast cell model), according to Ortega et al. (1991). For this, 4×10^6 PT18 cells or 1.2×10^5 RBL-2H3 cells (200 μL) were incubated in the presence of the peptides for 30 min in Tyrode's buffer at 37 °C/5% CO_2. After this, the cells were centrifuged and the supernatants collected. The cells incubated only with the Tyrode's buffer were lysed with 0.5% Triton X-100 (200 μL) (Sigma–Aldrich) solution to evaluate the total enzyme content. From each experimental sample to be assayed, four aliquots (10 μL) of the supernatant were taken to separate microwell plates. To these samples, 90 μL of the substrate solution containing 1.3 mg/mL of p-nitrophenyl-N-acetyl-β-D-glucosamine (Sigma) in 0.1 M citrate, pH 4.5, were added and the plates incubated for 12 h at 37°C. The reactions were stopped by addition of 100 μL of 0.2 M glycine solution, pH 10.7, and the optical density determined at 405 nm in an ELISA reader (Labsystems Multiskan Ex). The extent of secretion was expressed as the net percentage of the total β-hexosaminidase activity in the supernatant of unstimulated cells. The results represent the mean of quadruplicate tests ± standard deviation (SD).

2.10. Leishmanicidal activity

Medium 199 was used for the cultivation of promastigotes of *Leishmania major* (MHOM/SU/73/5ASKH). Promastigotes were cultured in the medium [supplemented with heat-inactivated (56 °C for 30 min) fetal bovine serum (10%)] at 27 °C, in a 5% CO_2 atmosphere in an incubator (Takahashi et al., 2004).

The leishmanicidal effects of the peptides were assessed using the improved 3-[4,5-dimethylthiazol-2-yl]-2,5-diphenyltetrasodium bromide (MTT) method as follows. Cultured promastigotes were seeded at 4×10^5/50 mL of the medium per well in 96-well microplates, and then 50 mL of different concentrations of test compounds dissolved in a mixture of DMSO and the medium were added to each well. Each concentration was tested in triplicate. The microplate was incubated at 27 °C in 5% CO_2 for 48 h. TetraColor ONE (10 mL) a mixture of 2-(2-methoxy-4-nitrophenyl)-3-(4-nitrophenyl)-5-(2,4-disulfophenyl)-2*H*-tetrazolium,monosodium salt and 1-methoxy-5-methylphenazinium methosulfate was added to each well and the plates were incubated at 27 °C for 6 h. Optical density values (test wavelength 450 nm; reference wavelength 630 nm) were measured using a microplate reader (Thermo BioAnalysis Japan Co., Ltd., Kanagawa, Japan). The values of 50% inhibitory concentration of the peptides were estimated from the dose–response curve.

Eumenitin	L**N**L**K**GIF**KK**VA**S**LL**T**
Eumenitin-R	L**N**L**K**GLI**KK**VA**S**LL**N**
Eumenitin-F	L**N**L**K**GLF**KK**VA**S**LL**T**
EMP-ER	F**D**IMGLI**KK**VAGAL-NH_2
EMP-EF	F**D**VMGII**KK**IA**S**AL-NH_2
EMP-AF	I**N**LL**K**IA**K**GII**KS**L-NH_2
HR-1	I**N**L**K**AIAALV**KK**VL-NH_2

Fig. 2. Amino acid sequences of the venom peptides from solitary eumenine wasp and HR-1 (Histamine Releasing peptide) from social wasp *Vespa orientalis* venom. Polar, charged residues are shown in bold types.

3. Results

3.1. Purification and sequence determination

The venom extracts of *E. rubrofemoratus* were subjected to reversed-phase HPLC, and the purity and complexity of each fraction was examined by MALDI-TOF MS. The HPLC profile was rather simple, having only several intense peaks (Fig. 1A). The two major fractions eluted at 26.1 and 27.6 min showed a high purity with protonated molecular ion peaks at *m/z* 1623.9 and 1474.9 (MH^+, monoisotopic), respectively. The molecular weight and chromatographic behavior suggested these components to be peptides, which we named eumenitin-R and eumenine mastoparan-ER (EMP-ER), respectively.

The sequence of the peptides was analyzed first by MALDI-TOF/TOF MS. Eumenitin-R had a sequence of 15 amino acids as I/L-N-I/L-K/Q-G-I/L-I/L-K/Q-K/Q-V-A-S-I/L-I/L-N, which was consistent with the observed molecular mass. However, contrary to expectation, there was no *d* or *w* ions observed, and therefore, no information about the I/L and K/Q differentiation. Accordingly, the sequence was determined by Edman degradation using an automated sequencer, giving whole sequence as L-N-L-K-G-L-I-K-K-V-A-S-L-L-N. The solid-phase synthesis of this peptide and the HPLC comparison of the synthetic specimen with the natural peptide finally corroborated the sequence.

The MALDI-TOF/TOF MS analysis of EMP-ER showed a 14 amino acid sequence with a C-terminal amide as F-D-I/L-M-G-I/L-I/L-K/Q-K/Q-V-A-G-A-I/L-NH_2, which was consistent with the observed molecular mass. However, there was again no information about the I/L differentiation. Edman degradation suggested a 13 amino acid sequence as F-D-I-M-G-L-I-K-K-V-A-G-A, and so, the C-terminal I/L was still

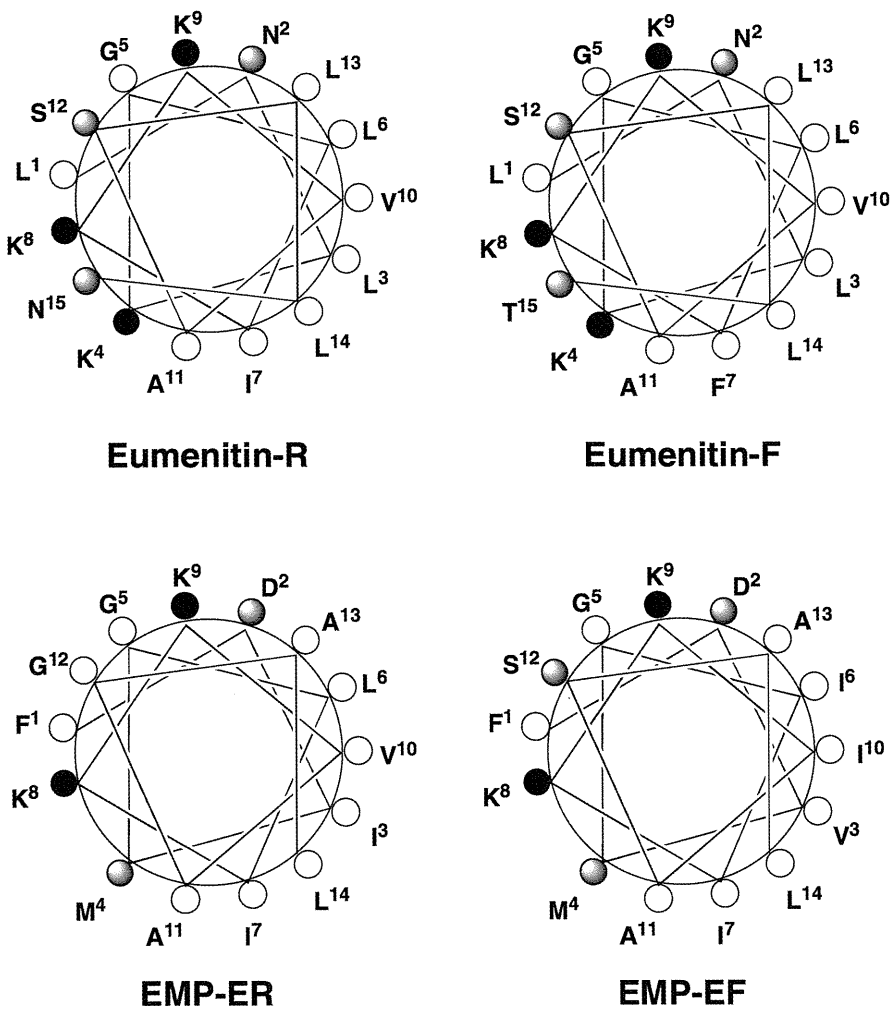

Fig. 3. Helical wheel projection of the sequences of the novel wasp venom peptides. In this view through the helix axis, the hydrophilic Ser (S), Thr (T), Asn (N) and Lys (K) residues are located on one side and the hydrophobic Ile (I), Leu (L) and Val (V) residues on the other side of the helix.

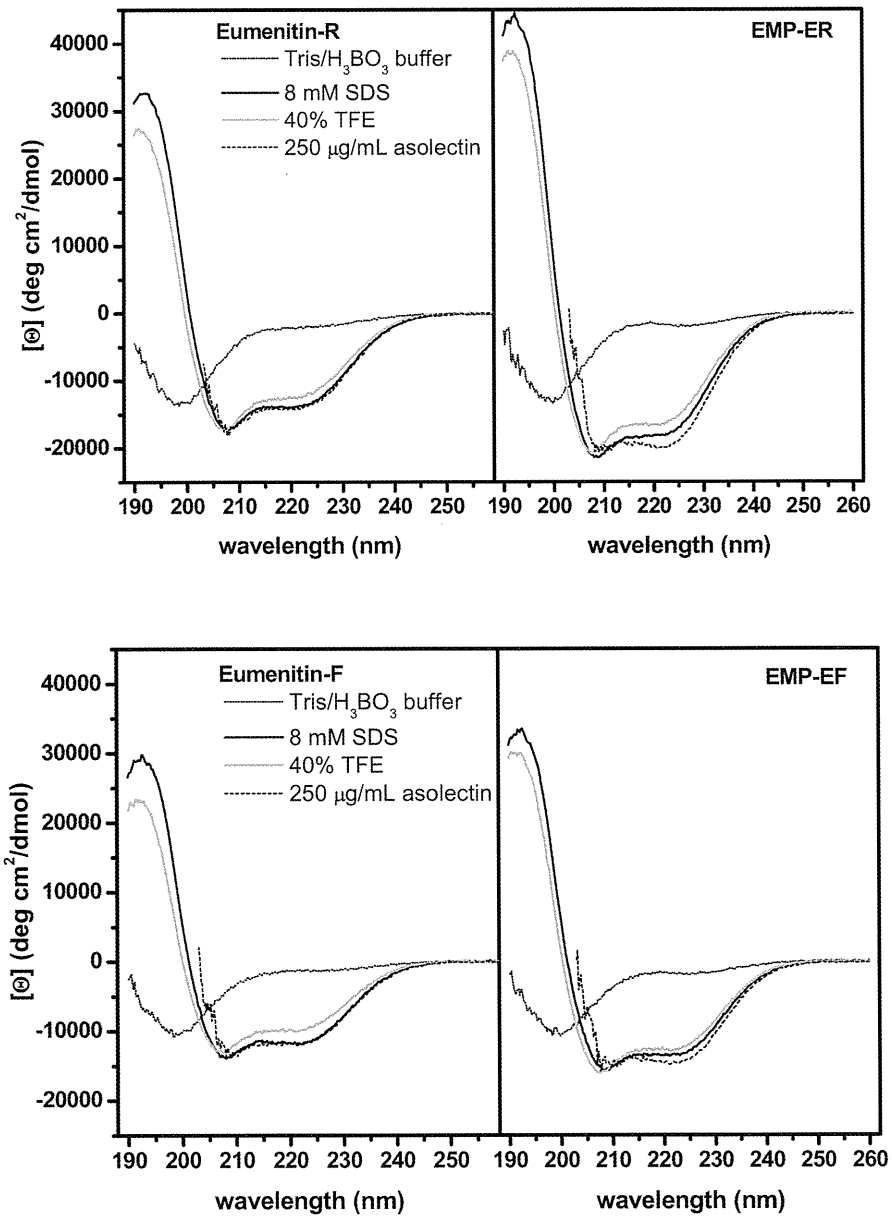

Fig. 4. CD spectra of the four peptides, eumenitin-R, EMP-ER, eumenitin-F and EMP-EF, obtained at 20 μM peptide concentration, at 25 °C in different environments. Peptides assume an α-helical conformation in 40% TFE, 8 mM SDS and in the presence of asolectin vesicles, showing modest preference for the anionic environments of SDS micelles and asolectin vesicles.

not determined. Finally, it was determined by the solid-phase synthesis of both the ^{14}I and ^{14}L peptides and their HPLC behavior was compared to the natural peptide. As a consequence, the ^{14}L peptide was found to be identical to the natural one, and therefore, the sequence was unambiguously determined as F-D-I-M-G-L-I-K-K-V-A-G-A-L-NH_2.

Similarly, eumenitin-F and eumenine mastoparan-EF (EMP-EF) were purified from the extracts of *E. fraterculus* (Fig. 1B), and in the same manner, the sequences were determined to be L-N-L-K-G-L-F-K-K-V-A-S-L-L-T and F-D-V-M-G-I-I-K-K-I-A-S-A-L-NH_2, respectively. The chemical features of these new peptides, rich in hydrophobic and basic amino acids with no disulfide bond, are characteristic of linear cationic cytolytic peptides (Kuhn-Nentwig, 2003), in particular, eumenitin-R and eumenitin-F, are highly homologous to eumenitin, whereas the other two, EMP-ER and EMP-EF, are similar to EMP-AF, thus can be classified as mastoparans (Fig. 2, Murata et al., 2009). This class of peptides has been known to adopt an amphipathic α-helical conformation, showing an amphiphilic character under appropriate conditions (Wakamatsu et al., 1992; Hori et al., 2001; Sforça et al., 2004; Todokoro et al., 2006).

The amphipaticity of peptides has been considered essential for their biological activities (Wimley, 2010). In fact, if the helical wheel projections of these peptide sequences were drawn, they show that amphipathic α-helical conformations could be possible as depicted in Fig. 3. Based on this view, all the hydrophilic amino acid residues, S, T, N and K, are located on one side, whereas the

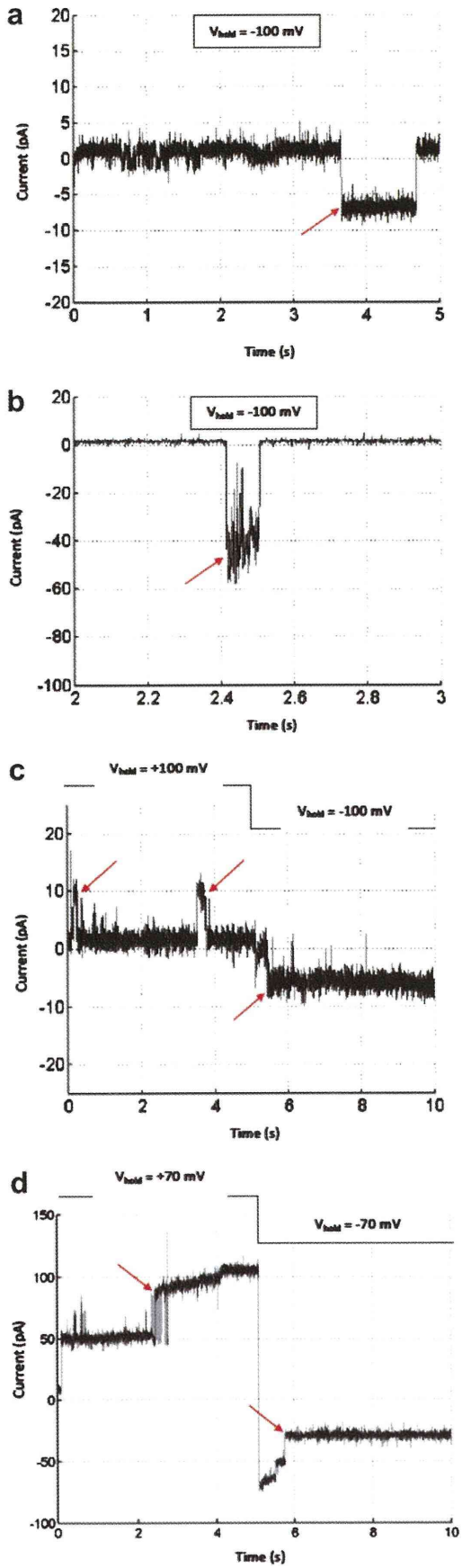

hydrophobic amino acid residues, I, L and V are on the other side of the helix.

3.2. CD spectroscopy

The Eumenine wasp venom peptides as well as mastoparan peptides are known to undergo a conformational change from a random coil to helical upon binding to lipid bilayers or in membrane mimetic environments (Park et al., 1995; dos Santos Cabrera et al., 2004; Konno et al., 2006). The α-helix content of these short chain peptides is directly related to favorable electrostatic interactions and the burial of the backbone into a more hydrophobic region. Fig. 4 shows the CD spectra of eumenitin-R, eumenitin-F, EMP-ER and EMP-EF obtained in different environments, to evaluate the relative importance of the electrostatic and hydrophobic contributions to the observed ellipticity. In water (spectra not shown) or in Tris/H_3BO_3 buffer, the spectra of the four peptides are equally characteristic of unordered structures, while assuming the features of an α-helical conformation with double minima around 208 and 222 nm in the membrane mimetic environments and in the presence of anionic asolectin vesicles (Fig. 4). The spectra acquired with 100 (not shown) and 250 μg/mL lipid contents, to check for further binding, showed a slight increase in the helical content (f_H), which for the four peptides is favored in the presence of anionic environments such as an 8 mM SDS solution or asolectin vesicles as already observed with EMP-AF (dos Santos Cabrera et al., 2004), eumenitin (Konno et al., 2006) and decoralin (Konno et al., 2007). These findings indicate that these helical peptides may present an amphipatic structure as determined for EMP-AF (Sforça et al., 2004) and mastoparans (Wakamatsu et al., 1992; Chuang et al., 1996; Hori et al., 2001; Todokoro et al., 2006).

3.3. Channel-like incorporation in mimetic lipid bilayers

The novel wasp venom peptides, at concentrations of 0.5–2 μM, induced an ion channel-like incorporation in lipid bilayers formed from the GUVs of asolectin (Figs. 5 and 6) under positive and negative voltage pulses, using a 150 mM HCl solution, within a 10 min incubation time. At peptide concentrations higher than 2 μM, the great number of incorporated channels (over 10) induced a breakdown of the lipid bilayers 2–3 s after applying our standard initial V_{hold} of −100 mV. The unitary channel conductances were determined at V_{hold} of +100 and −100 mV (see Table 2). Different levels were detected in different peptide sequences (Figs. 5 and 6), and only eumenitin-F and -R formed pores with conductances higher than 500 pS. From that we can assume that clusters can be formed and several units of the peptides organize to form bigger pores. Rectification was detected only in the eumenitin-F channels. Similar ion-channel like activity

Fig. 5. Single channel incorporation in asolectin lipid bilayers in the presence of the peptides eumenitin-R (a and b) and eumenitin-F (c and d) (0.5–2 μM). Solution: 150 mM HCl (symmetrical). Arrows indicate some channel apertures/closings. (a) Conductance 80 pS; (b) conductance = 410 pS; (c) the conductances were 81 pS (+100 mV) and 73 pS (−100 mV); (d) conductances were 190 and 885.7 pS (70 mV), and 238.6 and 332.9 pS (−70 mV).

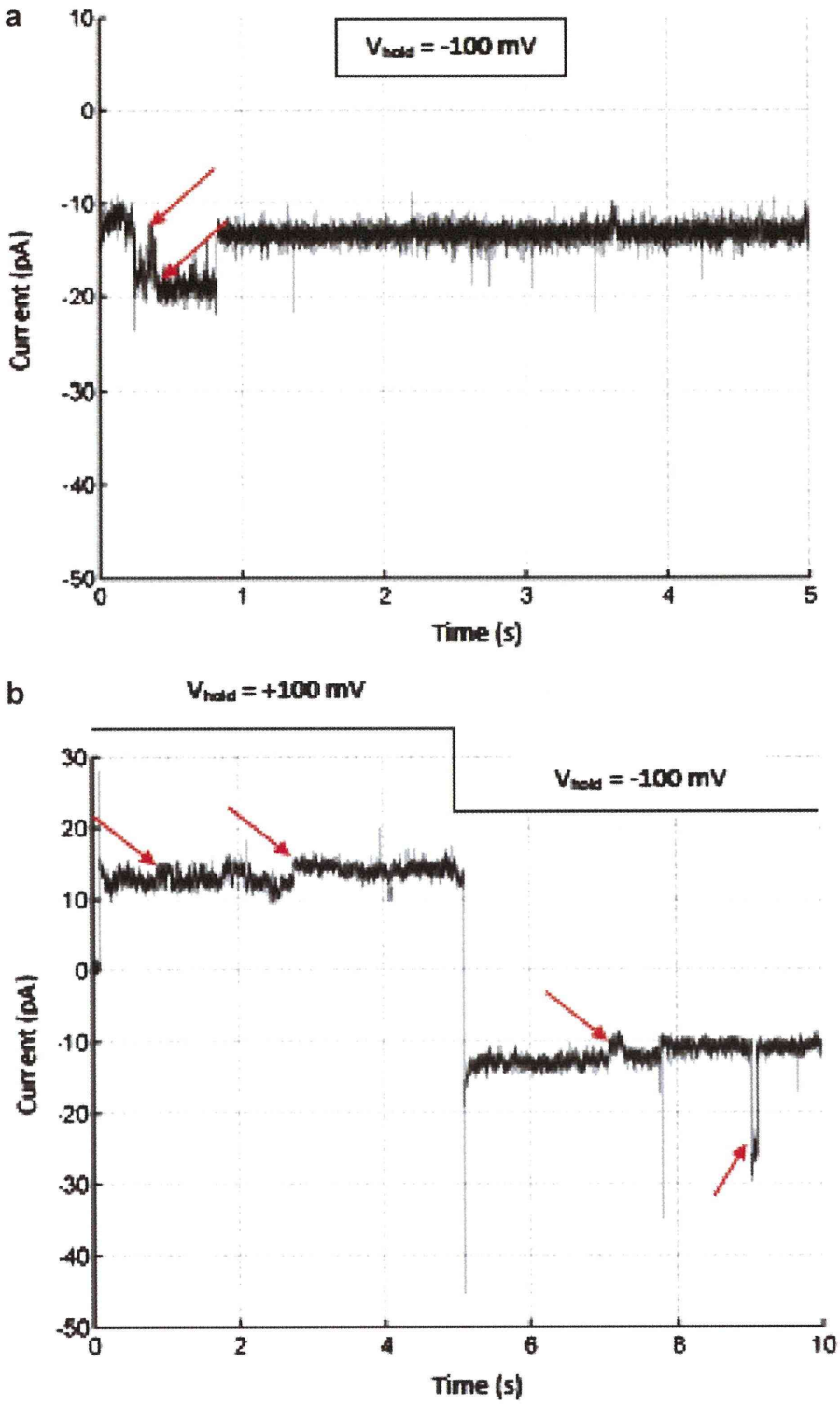

Fig. 6. Single channel incorporation in asolectin lipid bilayers in the presence of the peptides EMP-ER (a) and EMP-EF (b) (0.5–2 μM). Solution: 150 mM HCl (symmetrical). Arrows indicate some channel apertures. (a) Conductances were 28 and 60 pS; (b) conductances were 35 and 60 pS (+100 mV) and 35 and 75 pS (−100 mV).

was found with other peptides from solitary and social wasp venoms, as anoplin (dos Santos Cabrera et al., 2008), eumenitin (Arcisio-Miranda et al., 2008) and HR-1 (dos Santos Cabrera et al., 2009), as discussed below.

3.4. Biological activities

The mast cell degranulation, hemolysis, antimicrobial and antiprotozoan (leishmanicidal) activities were tested

Table 1
Structural and physicochemical properties of the new wasp venom peptides in comparison to eumenitin and mastoparan HR-1. Features shown are: number of amino acid residues in the sequence (N_{aa}), net charge (Q), hydrophobicity (H), time elapsed in the HPLC elution process, in minutes, and α-helix fraction (standard deviation ± 0.02).

	N_{aa}	Q[a]	H[b]	Elution time (min)	α-helix fraction		
					40% TFE	8 mM SDS	Asolectin
Eumenitin-R	15	+3	−0.034	26.1	0.43	0.48	0.49
EMP-ER	14	+2	0.131	27.6	0.53	0.59	0.65
Eumenitin-F	15	+3	−0.011	26.2	0.34	0.41	0.41
EMP-EF	14	+2	0.115	29.0	0.41	0.44	0.48
Eumenitin[c]	15	+3	0.002	Na	0.43	0.50[c]	na
Mast. HR1[d]	14	+4	0.067	Na	0.56	0.53	na

rc = random coil; na = unavailable.
[a] For peptides with an amidated C-terminus, includes an extra-charge.
[b] Calculated according to Eisenberg et al., consensus scale (1984).
[c] Konno et al., 2006.
[d] dos Santos Cabrera et al., 2009.

because these are characteristic biological activities for these types of peptide.

3.4.1. Antimicrobial activity

The peptide eumenitin-R was the most efficient in the antimicrobial assay, presenting the lowest MIC values against both Gram-positive and Gram-negative strains. Furthermore, all the peptides had more potent activities against the yeast *C. albicans* (Table 3). The four peptides described here showed an antimicrobial activity at very similar doses when compared to eumenitin (Konno et al., 2006).

3.4.2. Hemolytic activity

The solitary wasp peptides presented low to moderate hemolytic activities against mice erythrocytes in a dose-dependent manner (Fig. 7). A one-way analysis of variance (ANOVA) of the log EC_{50} (50% effective concentration) followed by the Newman–Keuls multiple comparison test indicated that EMP-ER and EMP-EF were more effective than eumenitin-R and eumenitin-F in this assay, presenting lower EC_{50} values (see Table 4 for EC_{50} values). Generally speaking, these peptides can be considered weakly hemolytic, especially eumenitin-R. These results well correlated with the hydrophobicity and shorter elution times of the respective peptides (see Table 1). The erythrocytes membranes show a zwitterionic character (Yeaman and Yount, 2003), and peptides with a lower charge and higher hydrophobicity present a stronger interaction with this type of membrane (de Souza et al., 2010).

Table 2
Mean, minimum and maximum conductances of anionic (AZO) bilayers induced by eumenine peptides according to the V_{hold} (3 different experiments).

Peptide	V_{hold} (mV)	Conductance (pS)	SEM	Minimum conductance (pS)	Maximum conductance (pS)
Eumenitin-R	−100	82.5	17.1	22	500
	+100	118.8	44	22	751
Eumenitin-F	−100	298.6	51	37	980
	+100	187.1	67.7	49	710
EMP-ER	−100	68.2	4	21	210
	+100	61.4	3.7	22	126
EMP-EF	−100	33.6	8.9	10	138
	+100	32.2	6.9	16	157

Table 3
Minimum inhibitory concentration (MIC) of the peptides from the wasps *Eumenes rubrofemoratus* (Eumenitin-R and EMP-ER) and *Eumenes fraterculus* (Eumenitin-F and EMP-EF), in μM.

Microorganism	Eumenitin-R	EMP-ER	Eumenitin-F	EMP-EF
Gram-positive				
Staphylococcus aureus ATCC 25923	60	30	>60	30
Staphylococcus epidermidis (clinical sample)	30	30	30	30
Micrococcus luteus ATCC 10240	15	>30	30	30
Streptococcus pyogenes (clinical sample)	15	>30	30	>30
Bacillus subtilis ATCC 6633	7.5	30	30	30
Gram-negative				
Escherichia coli ATCC 25922	30	30	30	30
Proteus mirabilis (clinical sample)	60	60	>60	60
Pseudomonas aeruginosa ATCC 27853	30	>30	30	>30
Stenotrophomonas maltophilia ATCC 13637	15	>30	15	>30
Yeast				
C. albicans ATCC 90112	<7.5	7.5	7.5	7.5

3.4.3. Mast cell degranulation

The ability of the peptides to induce mast cells degranulation was assayed *in vitro* in PT18 cells and RBL-2H3 cells, by the measurement of the enzyme β-hexosaminidase released. As shown in Fig. 8A, all the new peptides were able to induce mild degranulation in connective tissue-type mast cells with equivalent potencies and dose-dependent, similarly to Eumenitin, and weaker than mastoparan (Konno et al., 2006). On the other hand, in mucosal-type mast cells EMP-ER and EMP-EF, which are similar to EMP-AF, exhibited more intense mast cell degranulation than eumenitin-R and eumenitin-F, which are highly homologous to eumenitin (Fig. 8B).

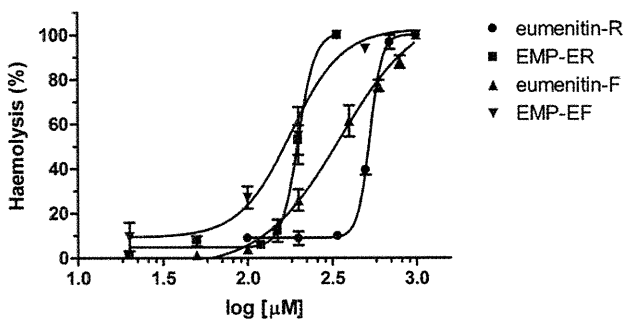

Fig. 7. The dose–response curves of the hemolytic activity of the wasp venom peptides in mouse erythrocytes show a dose-dependent relation. More hydrophilic peptides, eumenitin-R and eumenitin-F, present higher EC_{50} values. See also Table 3.

Table 4
Effective concentration (EC_{50}) of hemolytic activity of the wasp peptides and the 95% confidence intervals (CI), in μM ($n = 4$).

Peptide	EC_{50} (μM)	95% CI
Eumenitin-R	530.3	512.9 to 548.3
EMP-ER	200.0	189.6 to 211.0
Eumenitin-F	353.4	251.7 to 496.3
EMP-EF	181.1	142.6 to 229.9

3.4.4. *Leishmanicidal activity*

The results of the leishmanicidal assay are summarized in Table 5. For comparison, eumenitin and EMP-AF were also tested. Most peptides showed an activity, but only moderately. It is noteworthy that the eumenitin series (C-terminal free) are weaker than the EMP series (C-terminal amide). This is similar to our previous results of decoralin (C-terminal free) *vs.* decoralin-NH_2 (C-terminal amide) (Konno et al., 2007).

4. Discussion

In the present study, we have purified four new linear cationic α-helical peptides from two species of the eumenine solitary wasps, *E. rubrofemoratus* and *E. fraterculus*, and characterized them both chemically and biologically. Of these, eumenitin-R and eumenitin-F are highly homologous to eumenitin, whereas the others, eumenine mastoparan-ER (EMP-ER) and eumenine-mastoparan-EF (EMP-EF), are similar to EMP-AF, and thus, can be classified into mastoparan peptides. These results suggested that these types of peptide are commonly and widely distributed in the eumenine wasp venoms. All these peptides and anoplin present the following common interesting physicochemical and biological features: short chain length – 10 to 15 residues long, polycationic character, they assume α-helical conformation upon contact with membrane mimetic environments, and they are antimicrobial, hemolytic and mast cell degranulators at various levels.

Conformational and pore-forming activity of these new peptides were investigated in asolectin bilayers, which due to its anionic character mimic the cytoplasmic membrane of bacteria. This phospholipid, whose approximate composition is 23.5% phosphatidylcholine, 20% phosphatidylethanolamine, and 14% inositol phosphatides (other components are 39.5% other phospholipids, lipids and carbohydrates, and 2% triglycerides, tocopherols, sterols), holds some similarities to the lipid composition of rat mast cells; the phospholipids amount roughly to 50% of the total lipids, from these phosphatidylcholine is 30%, phosphatidylethanolamine 27%, sphingomyelin 20%, and phosphatidylserine and phosphatidylinositol are 16%. An important difference lies in that cholesterol represent around 20% of the total lipids content in rat mast cell membranes, while in asolectin sterols, it represents less than 0.3% (Strandberg and Westerberg, 1976). In relation to sterols and the general anionic character, this bilayer can also be considered a mimetic of microbial membranes. Thus the behavior of these new Eumenine peptides can be reasonably well modeled and their mechanism of action understood through the use of asolectin bilayers.

Peptides such as mastoparans adopt an amphipatic α-helical conformation in anisotropic or membrane mimetic media (Wakamatsu et al., 1992; Chuang et al., 1996; Hori et al., 2001; Sforça et al., 2004; Todokoro et al., 2006). Similarly the four peptides in our study presented circular dichroism spectra that are characteristic of helical structures with practically equivalent α-helix content, except for EMP-ER, which showed a higher helical content.

The experiments of electrical measurements in planar lipid bilayers of anionic asolectin showed that all the new peptides present a pore- or channel-like activity, in both the positive and negative voltage pulses, as previously demonstrated for eumenitin (Arcisio-Miranda et al., 2008), anoplin (dos Santos Cabrera et al., 2008) and other mastoparan peptides (Mellor and Sansom, 1990; dos Santos Cabrera et al., 2009). Channels with lower and higher conductance levels were recorded, but the latter ones were less frequent, and formed only in the presence of the non-amidated C-terminal peptides (eumenitin-R and eumenitin-F).

The channel-like activity of these peptides is similar to that observed with eumenitin in the same lipid bilayer as

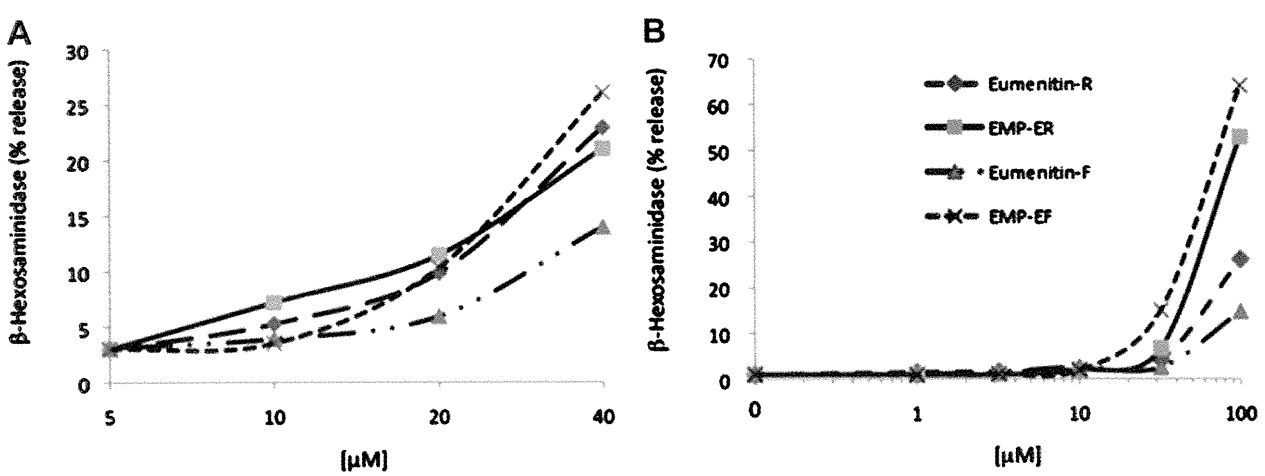

Fig. 8. The degranulation in PT18 cells (A: a connective tissue-type mast cell model) and RBL-2H3 cells (B: a mucosal-type mast cell model) measured by the β-hexosaminidase release, basal and after treatment with the peptides from the wasps *Eumenes rubrofemoratus* (eumenitin-R and EMP-ER) and *Eumenes fraterculus* (eumenitin-F and EMP-EF). Concentrations are in μM (values inside parentheses). Data represent the mean from 2–4 independent experiments.

Table 5
Leishmanicidal activity of the wasp venom peptides.

Peptide	IC_{50} (μM)[a]
Eumenitin	35
Eumenitin-R	>62
Eumenitin-F	52
EMP-ER	20
EMP-EF	40
EMP-AF	35
Amphotericin B[b]	<0.1

[a] IC_{50}: 50% inhibitory concentration.
[b] Used as positive control.

could be foreseen from the high homology in their respective sequences. However, eumenitin-F channels presented strong rectification under negative voltage pulses, similarly to the mastoparan peptide HR-1 pores, whose conductances were nearly four times higher when the V_{hold} was changed to negative pulses (dos Santos Cabrera et al., 2009).

Concerning EMP-ER and EMP-EF, their pore conductance levels are equivalent to those for mastoparan HR-1, although they present a lower degree of homology, different net charges and different hydrophobicities (Fig. 2 and Table 1). These physicochemical differences could account for the double conductance levels found with EMP-ER and EMP-EF, which were not detected in HR-1 (dos Santos Cabrera et al., 2009).

Overall, the electrophysiology results confirmed the lytic activity of these new peptides. Short chain peptides, shorter than the bilayer thickness, made of bulky residues and showing pore-like activity combine characteristics that favor the toroidal pore model (Matsuzaki et al., 1996; Yang et al., 2001), by which the pore is described as a complex made of lipid molecules, predominantly, and peptide molecules that induced the bilayer destabilization by inserting into it. Models describing peptide membrane interactions have recently been determined as not reflecting static structures to which one or multiple peptide monomers contribute (Quian et al., 2008; Marsh, 2009; Leontiadou et al., 2006; Herce and Garcia, 2007). Additional experiments to describe the mechanisms of pore formation, besides the preliminary results described herein, are currently ongoing in our laboratories. Based on the bioassays performed with the synthetic peptides, their antimicrobial, leishmanicidal and cytolytic properties were determined. The leishmanicidal activity of the peptides was detected in concentrations similar or slightly higher than the antimicrobial activity, and EMP-ER presented the strongest inhibition of the *L. major* promastigotes. This activity was dependent of the C-terminal amide, in a way similar to the results with decoralin *vs.* decoralin-NH_2 (Konno et al., 2007). All four peptides induced mast cell degranulation in a dose-dependent manner with similar potencies. The peptides were also hemolytic against mouse erythrocytes, but in higher concentrations than those used in the antimicrobial assays. The peptides eumenitin-R and eumenitin-F showed a weak hemolytic activity, probably because of the low hydrophobicity, in a way similar to eumenitin (Konno et al., 2006) or also due to the lack of the C-terminal amide modification as in EMP-AF1 (dos Santos Cabrera et al., 2004). Furthermore, the peptides eumenitin-R and to a similar extent eumenitin-F, presented the strongest antimicrobial activity, which could be attributed to their higher net charges (Dathe and Wieprecht, 1999; Dathe et al., 2002). All four peptides inhibited the growth of the yeast *C. albicans* at low concentrations, and again we emphasize the eumenitin-R activity.

Based on these results, eumenitin-R appears as the peptide showing higher potential as a leading compound in drug development. Like eumenitin it associates an average net charge and low hydrophobicity, which resulted in an interesting antimicrobial activity, mainly considering clinical samples, and practically devoid of undesirable effects as hemolytic and mast cell degranulating activities.

Conflict of interest

The authors declare that there are no conflicts of interest.

Acknowledgements

The authors thank Dr. Christoph Borchers, Facility Director of the University of Victoria Proteomics Centre, Canada, for the cooperation on the peptides synthesis and Prof. Dr. João Ruggiero Neto for the use of the CD equipment and the laboratory facilities. This work was supported by FAPESP – Fundação de Amparo à Pesquisa do Estado de São Paulo, Brazil (2008/00173-4), CNPq – Conselho Nacional de Desenvolvimento Científico e Tecnológico, Brazil (307457/2008-7); MPSC acknowledges the support of CNPq (477507/2008-5).

References

Arcisio-Miranda, M., Cabrera, M.P.S., Konno, K., Rangel, M., Procopio, J., 2008. Effects of the cationic antimicrobial peptide Eumenitin from the venom of solitary wasp Eumenes rubronotatus in planar lipid bilayers: surface charge and pore formation activity. Toxicon 51, 736–745.

Chuang, C.C., Huang, W.C., Yu, H.M., Wang, K.T., Wu, S.H., 1996. Conformation of *Vespa basalis* mastoparan-B in trifluoroethanol-containing aqueous solution. Biochim. Biophys. Acta 1292, 1–8.

Dathe, M., Wieprecht, T., 1999. Structural features of helical antimicrobial peptides: their potencial to modulate activity on model membranes and biological cells. Biochim. Biophys. Acta 1462, 71–87.

Dathe, M., Meyer, J., Beyermann, M., Maul, B., Hoischen, C., Bienert, M., 2002. General aspects of peptide selectivity towards lipid bilayers and cell membranes studied by variation of the structural parameters of amphipathic helical model peptides. Biochim. Biophys. Acta 1558, 171–186.

Eisenberg, D., Schwarz, E., Komaromy, M., Wall, R., 1984. Analysis of membrane and surface protein sequences with the hydrophobic moment plot. J. Mol. Biol. 179, 125–142.

Eldefrawi, A.T., Eldefrawi, M.E., Konno, K., Mansour, N.A., Nakanishi, K., Oltz, E., Usherwood, P.N.R., 1988. Structure and synthesis of a potent glutamate receptor antagonist in wasp venom. Proc. Natl. Acad. Sci. U S A 85, 4910–4913.

Fertig, N., Blick, R.H., Behrends, J.C., 2002. Whole cell patch clamp recording performed on a planar glass chip. Biophys. J. 82, 3056–3062.

Herce, H., Garcia, A.E., 2007. Molecular dynamics simulations suggest a mechanism for translocation of the HIV-1 TAT peptide across lipid membranes. Proc. Natl. Acad. Sci. U S A 104, 20805–20810.

Hori, Y., Demura, M., Iwadate, M., Ulrich, A.S., Niidome, T., Aoyagi, H., Asakura, T., 2001. Interaction of mastoparan with membranes studied by 1H-NMR spectroscopy in detergent micelles and by solid-state 2H-NMR and 15N-NMR spectroscopy in oriented lipid bilayers. Eur. J. Biochem. 268, 302–309.

Konno, K., Hisada, M., Miwa, A., Itagaki, Y., Naoki, H., Kawai, N., Yasuhara, T., Takayama, H., 1998. Isolation and structure of

pompilidotoxins (PMTXs), novel neurotoxins in solitary wasp venoms. Biochem. Biophys. Res. Commun. 250, 612–616.
Konno, K., Hisada, M., Naoki, H., Itagaki, Y., Kawai, N., Miwa, A., Yasuhara, T., Morimoto, Y., Nakata, Y., 2000. Structure and biological activities of eumenine mastoparan-AF (EMP-AF), a novel mast cell degranulating peptide in the venom of the solitary wasp *Anterhynchium flavomarginatum micado*. Toxicon 38, 1505–1515.
Konno, K., Hisada, M., Fontana, R., Lorenzi, C.C.B., Naoki, H., Itagaki, Y., Miwa, A., Kawai, N., Nakata, Y., Yasuhara, T., Ruggiero Neto, J., de Azevedo, W.F., Palma, M.S., Nakajima, T., 2001. Anoplin, a novel antimicrobial peptide from the venom of the solitary wasp *Anoplius samariensis*. Biochim. Biophys. Acta 1550, 70–80.
Konno, K., Hisada, M., Naoki, H., Itagaki, Y., Fontana, R., Rangel, M., Oliveira, J.R., Cabrera, M.P.S., Ruggiero Neto, J., Hide, I., Nakata, Y., Yasuhara, T., Nakajima, T., 2006. Eumenitin, a novel antimicrobial peptide from the venom of the solitary eumenine wasp *Eumenes rubronotatus*. Peptides 27, 2624–2631.
Konno, K., Rangel, R., Oliveira, J.S., Cabrera, M.P.S., Fontana, R., Hirata, I.Y., Hide, I., Nakata, Y., Mori, K., Kawano, M., Fuchino, H., Sekita, S., Ruggiero Neto, J., 2007. Decoralin, a novel linear cationic α-helical peptide from the venom of the solitary eumenine wasp *Oreumenes decoratus*. Peptides 28, 2320–2327.
Kuhn-Nentwig, L., 2003. Antimicrobial and cytolytic peptides of venomous arthropods. Cell. Mol. Life Sci. 60, 2651–2668.
Leontiadou, H., Mark, A.E., Marrink, S.J., 2006. Antimicrobial peptides in action. J. Am. Chem. Soc. 128, 12156–12161.
Marsh, D., 2009. Orientation and peptide-lipid interactions of alamethicin incorporated in phospholipid membranes: polarized infrared and spin-label EPR spectroscopy. Biochemistry 48, 729–737.
Matsuzaki, K., Murase, O., Fujii, N., Miyajima, K., 1996. An antimicrobial peptide, magainin 2, induced rapid flip-flop of phospholipids coupled with pore formation and peptide translocation. Biochemistry 35, 11361–11368.
Mellor, I.R., Sansom, M.S., 1990. Ion-channel properties of mastoparan, a 14-residue peptide from wasp venom, and of MP3, a 12-residue analogue. Proc. R. Soc. Lond. B Biol. Sci. 239, 383–400.
Murata, K., Shinada, T., Ohfune, Y., Hisada, M., Yasuda, A., Naoki, H., Nakajima, T., 2009. Novel mastoparan and protonectin analogs isolated from a solitary wasp, *Orancistrocerus drewseni drewseni*. Amino Acids 37, 389–394.
Ortega, E., Schneider, H., Pecht, I., 1991. Possible interactions between the Fc epsilon receptor and a novel mast cell function-associated antigen. Int. Immunol. 3, 333–342.
Park, N.G., Yamato, Y., Lee, S., Sugihara, G., 1995. Interaction of mastoparan-B from venom of a hornet in Taiwan with phospholipid bilayers and its antimicrobial activity. Biopolymers 36, 793–801.
Prates, M.V., Sforça, M.L., Regis, W.C.B., Leite, J.R.S.A., Silva, L.P., Pertinhez, T.A., Araújo, A.L.T., Azevedo, R.B., Spisni, A., Bloch Jr., C., 2004. The NMR-derived solution structure of a new cationic antimicrobial peptide from the skin secretion of the anuran *Hyla punctata*. J. Biol. Chem. 279, 13018–13026.
Quian, S., Wang, W., Yang, L., Huang, H.W., 2008. Structure of transmembrane pore induced by bax-derived peptide: evidence for lipidic pores. Proc. Natl. Acad. Sci. U S A 105, 17379–17383.
Rangel, M., Malpezzi, E.L.A., Ssusini, S.M.M., Freitas, J.C., 1997. Hemolytic activity in extracts of the diatom *Nitzschia*. Toxicon 35, 305–309.
Rohl, C.A., Baldwin, R.L., 1998. Deciphering rules of helix stability in peptides. Meth. Enzymol. 295, 1–26.
dos Santos Cabrera, M.P., Souza, B.M., Fontana, R., Konno, K., Palma, M.S., de Azevedo, W.F., Ruggiero Neto, J., 2004. Conformation and lytic activity of eumenine mastoparan: a new antimicrobial peptide from wasp venom. J. Pept. Res. 64, 95–103.
dos Santos Cabrera, M.P., Arcisio-Miranda, M., Costa, S.T.B., Konno, K., Ruggiero Jr., , Procopio, J., Ruggiero Neto, J., 2008. Study of the mechanism of action of anoplin, a helical antimicrobial decapeptide with ion channel-like activity, and the role of the amidated C-terminus. J. Pept. Sci. 14, 661–669.
dos Santos Cabrera, M.P., Arcisio-Miranda, M., da Costa, L.C., de Souza, B. M., Costa, S.T.B., Palma, M.S., Ruggiero Neto, J., Procopio, J., 2009. Interactions of mast cell degranulating peptides with model membranes: a comparative biophysical study. Arch. Biochem. Biophys. 486, 1–11.
Sforça, M.L., Oyama Jr., S., Canduri, F., Lorenzi, C.C.B., Pertinhez, T.A., Konno, K., Souza, B.M., Palma, M.S., Ruggiero Neto, J., de Azevedo Jr., W.F., Spisni, A., 2004. How C-terminal carboxyamidation alters the biological activity of peptides from the venom of the eumenine solitary wasp. Biochemistry 43, 5608–5617.
Sondermann, M., George, M., Fertig, N., Behrends, J.C., 2006. High-resolution electrophysiology on a chip: transient dynamics of alamethicin channel formation. Biochim. Biophys. Acta 1758, 545–551.
de Souza, B.M., dos Santos Cabrera, M.P., Ruggiero Neto Jr., J., Palma, M.S., 2010. Investigating the effect of different positioning of lysine residues along the peptide chain of mastoparans for their secondary structures and biological activities. Amino Acids. doi:10.1007/s00726-010-0481-y.
Strandberg, K., Westerberg, S., 1976. Composition of phospholipids and phospholipid fatty acids in rat mast cells. Mol. Cell. Biochem. 11, 103–107.
Takahashi, M., Fuchino, H., Satake, M., Agatsuma, Y., Sekita, S., 2004. In vitro screening of leishmanicidal activity of Myanmar timber extracts. Biol. Pharm. Bull. 27, 921–925.
Todokoro, Y., Yumen, I., Fukushima, K., Kang, S.-W., Park, J.S., Kohno, T., Wakamatsu, K., Akutsu, H., Fujiwara, T., 2006. Structure of tightly membrane-bound mastoparan-X, a G-protein-activating peptide, determined by solid-state NMR. Biophys. J. 91, 1368–1379.
Wakamatsu, K., Okada, A., Miyazawa, T., Ohya, M., Higashijima, T., 1992. Membrane-bound conformation of mastoparan-X, a G protein-activating peptide. Biochemistry 3, 5654–5660.
Wayne, P.A., 2004. NCCLS. Performance Standards for Antimicrobial Susceptibility Testing; Fourteenth Informational Supplement, vol. 24(1). National Committee of Clinical Laboratory Standards. NCCLS document M100–S14.
Wimley, W.C., 2010. Describing the mechanism of antimicrobial peptide action with the interfacial activity model. ACS Chem. Biol. 5, 905–917.
Yamamoto, T., Arimoto, H., Kinumi, T., Oba, Y., Uemura, D., 2007. Identification of proteins from venom of the paralytic spider wasp, *Cyphononyx dorsalis*. Insect Biochem. Mol. Biol. 37, 278–286.
Yang, L., Harroun, T.A., Weiss, T.M., Ding, L., Huang, H.W., 2001. Barrel-stave model or toroidal model? A case study on melittin pores. Biophys. J. 81, 1475–1485.
Yasuhara, T., Mantel, P., Nakajima, T., Piek, T., 1987. Two kinins isolated from an extract of the venom reservoirs of the solitary wasp *Megascolia flavifrons*. Toxicon 25, 527–535.
Yeaman, M.R., Yount, N.Y., 2003. Mechanisms of antimicrobial peptide action and resistance. Pharmacol. Rev. 55, 27–56.